ORIGINAL PAPER

The membrane potential arising from the adsorption of ions at the biological interface

Hirohisa Tamagawa[1] · Bernard Delalande[2]

Abstract

Membrane theory makes it possible to compute the membrane potential of living cells accurately. The principle is that the plasma membrane is selectively permeable to ions and that its permeability to mobile ions determines the characteristics of the membrane potential. However, an artificial experimental cell system with an impermeable membrane can exhibit a nonzero membrane potential, and its characteristics are consistent with the prediction of the Goldman–Hodgkin–Katz eq., which is a noteworthy concept of membrane theory, despite the membrane's impermeability to mobile ions. We noticed this troublesome facet of the membrane theory. We measured the potentials through permeable and impermeable membranes where we used the broad varieties of membranes. Then we concluded that the membrane potential must be primarily, although not wholly, governed by the ion adsorption-desorption process rather than by the passage of ions across the cell membrane. A theory based on the Association-Induction Hypothesis seems to be a more plausible mechanism for the generation of the membrane potential and to explain this unexpected physiological fact. The Association-Induction Hypothesis states that selective ion permeability of the membrane is not a condition for the generation of the membrane potential in living cells, which contradicts the prediction of the membrane theory. Therefore, the Association-Induction Hypothesis is the actual cause of membrane potential. We continued the theoretical analysis by taking into account the Association-Induction Hypothesis and saw that its universality as a cause of potential generation mechanism. We then concluded that the interfacial charge distribution is one of the fundamental causes of the membrane potential.

Keywords Membrane potential · Membrane theory · Goldman–Hodgkin–Katz equation · Permeability coefficient · Association-Induction Hypothesis · Ion adsorption-desorption · Surface charge density · Interface

Introduction

Membrane theory suggests that the passage of mobile ions across the plasma membrane causes the membrane potential. On the other hand, our previous works indicate that the cause of the membrane potential is the heterogeneous charge distribution caused by the spatial fixation of mobile ions governed by the mass action law (ion adsorption-desorption)

✉ Hirohisa Tamagawa
   tmgwhrhs@gifu-u.ac.jp

   Bernard Delalande
   bernard@somasimple.com

1   Department of Mechanical Engineering, Faculty of Engineering, Gifu University, 1-1 Yanagido, Gifu 501-1193, Japan

2   280 avenue de la Pierre Dourdant, 38290 La Verpilliere, France

(Tamagawa and Ikeda 2018; Tamagawa 2018; Tamagawa et al. 2021a, b). This outcome was originally proposed by Ling more than a half century ago in his own theory of the Association-Induction Hypothesis (abbreviated by AIH), (Ling 1992; Ling 1997; Ling 2001, Ling 2007). It is a long-dismissed physiological theory, but we have pointed out that AIH is a more plausible theory than membrane theory for explaining the cause of membrane potential generation, and we have no rational reasons to exclude AIH as an alternative to membrane theory.

The Goldman–Hodgkin–Katz equation (GHK eq.) is believed to accurately predict the resting potential (Ling 1992; Ling 1997; Ling 2001; Ling 2007; Cronin 1987; Keener and Sneyd 2008; Ermentrout and Terman 2010). It suggests that the membrane permeability to the individual mobile ions governs the resting potential. The GHK eq. is even used to discuss the pattern of the action potential. The generation of action potentials is often attributed to the

change in cell membrane permeability to mobile ions. Equation 1 is a typical GHK eq. that computes the membrane potential when the Na^+, K^+ and Cl^- exist in the cell system as mobile ions. L and R in Eq. 1 represent cell-interior and cell-exterior, respectively, in this case.

$$\phi = -\frac{kT}{e} \ln \frac{P_{Na}[Na^+]_L + P_K[K^+]_L + P_{Cl}[Cl^-]_R}{P_{Na}[Na^+]_R + P_K[K^+]_R + P_{Cl}[Cl^-]_L} \quad (1)$$

P_i : permeability coefficient to the ion i

Eq. 1 is based on an almost plausible mechanism of membrane potential generation, and it can provide the membrane potential in accurate agreement with the experimentally measured membrane potential. However, another theory based on AIH leads to another mathematical formula represented by Eq. 2 (Tamagawa and Ikeda 2018). Although Eq. 2 looks the same as Eq. 1, its physiological meaning is totally different from Eq. 1. K_i is an association constant, while P_i of Eq. 1 is a permeability coefficient. The foundation of Eq. 1 lies in the membrane permeability to ions, while that of Eq. 2 lies in the ion adsorption-desorption (association-dissociation). Our previous work suggests that Eq. 2 appears to have broader applicabilities to the experimental fact, and eventually the AIH which is the foundation of Eq. 2 was suggested to be a more plausible physiological theory than membrane theory (Tamagawa and Ikeda 2018; Tamagawa 2018; Tamagawa et al. 2021a, b). Nevertheless, the AIH is still unknown to the scientific community and the objection to the AIH is by far prevailing compared with the membrane theory. We will discuss the origin of the membrane potential here again using fairly simple but broad variety of experimental systems and a simple theoretical analysis in this work. Then we will see the universality of AIH.

$$\phi = -\frac{kT}{e} \ln \frac{K_{Na}[Na^+]_L + K_K[K^+]_L + K_{Cl}[Cl^-]_R}{K_{Na}[Na^+]_R + K_K[K^+]_R + K_{Cl}[Cl^-]_L}$$

K_i : association constant of the ion i with its adsorption site

$$(2)$$

Issues to be addressed

Before moving on to the explanation of our experimental work and theoretical discussion, we would like to clarify our questioning and how we answered it.

What is the purpose of the Goldman–Hodgkin–Katz equation?

GHK eq. can compute the experimentally measured membrane potential quite precisely. GHK eq. indicates that plasma membrane permeability governs the membrane potential, and the plasma membrane permeability to

the mobile ions is usually represented by "P_i" as in Eq. 1. However, usually P_i is not experimentally determined, but rather estimated so that the GHK eq. can reproduce the potentials measured in the experiment as to be touched upon in Sect. 4.1 as well (Tamagawa and Ikeda 2018; Wright and Diamond 1968; Olschewski et al. 2001; Uteshev 2010). It is always possible to choose P_i so that the GHK eq. can reproduce the given potential data. For example, imagine a cell system immersed in an electrolyte solution. Given that K^+, Na^+, and Cl^- account for most of the ions in the system, the membrane potential is given by Eq. 1 of course. Given that all ion concentrations and membrane potentials are experimentally known, it is easy to find P_i that mathematically satisfy the GHK eq. even if P_i is experimentally unknown. In this case, the total number of suitable P_i must be almost infinite, but these P_i's cannot represent the real permeability coefficients. Such P_i's are the arbitrary parameters that allow us to associate the experimental potential and the potential calculated from the GHK eq., which may have no physiological meaning (Tamagawa and Ikeda 2018).

Let us now consider a slightly more complex case. Imagine a cell immersed in an electrolytic solution. We then assume that Na^+, K^+, and Cl^- represent virtually all the ions in the system. When the ion concentration of the cell-exterior is varied, say the concentration of KCl is varied and the cell-interior concentration is kept constant, the experimentally measured membrane potential generally behaves as indicated by the symbols "○" in Fig. 1.

The membrane potential shows an almost straight line with a slope of $+kT/e$ (or $-kT/e$) against the cell-exterior ionic concentration, while the variation of the membrane potential becomes indifferent to the variation of the ionic concentration in the low ionic concentration range. Such a membrane potential behaviour is quite typical (Tamagawa et al. 2021a; Hodgkin and Howrowicz 1959; Diamond and Harrison 1966; Moreton 1968; Shinagawa 1976; Chang 1983; Zhang and Wakamatsu 2002). Even in this somewhat
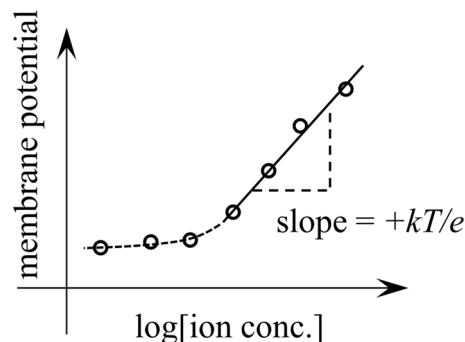

Fig. 1 Membrane potential vs. cell-exterior ion concentration. The horizontal axis represents the logarithm of cell-exterior ion concentration whose concentration is varied

complex case, the membrane potential is usually considered by Eq. 1. Calculating such a membrane potential profile using the GHK eq. is not at all difficult. The membrane potential profiles can be explained qualitatively as follows: Eq. 1 is transformed by Eq. 3.

$$
\begin{aligned}
\phi &= -\frac{kT}{e}ln\left[\frac{P_{\text{Na}}[\text{Na}^+]_L + P_{\text{K}}[\text{K}^+]_L + P_{\text{Cl}}[\text{Cl}^-]_R}{P_{\text{Na}}[\text{Na}^+]_R + P_{\text{K}}[\text{K}^+]_R + P_{\text{Cl}}[\text{Cl}^-]_L}\right] \\
&= -\frac{kT}{e}ln\left[P_{\text{Na}}[\text{Na}^+]_L + P_{\text{K}}[\text{K}^+]_L + P_{\text{Cl}}[\text{Cl}^-]_R\right] \\
&\quad + \frac{kT}{e}ln\left[P_{\text{Na}}[\text{Na}^+]_R + P_{\text{K}}[\text{K}^+]_R + P_{\text{Cl}}[\text{Cl}^-]_L\right] \\
&= -\frac{kT}{e}ln\left[C_n + P_{\text{Cl}}[\text{Cl}^-]_R\right] + \frac{kT}{e}ln\left[P_{\text{K}}[\text{K}^+]_R + C_d\right]
\end{aligned}
$$
$$
C_n \equiv P_{\text{Na}}[\text{Na}^+]_L + P_{\text{K}}[\text{K}^+]_L, \quad C_d \equiv P_{\text{Na}}[\text{Na}^+]_R + P_{\text{Cl}}[\text{Cl}^-]_L \tag{3}
$$

In Eq. 3, C_n and C_d are considered virtually constant. Hence, the controllable quantities are only $[\text{K}^+]_R$ and $[\text{Cl}^-]_R$. Then, of course $[\text{K}^+]_R = [\text{Cl}^-]_R$. Therefore, Eq. 3 is given by Eq. 4.

$$
\phi(Z) = -\frac{kT}{e}ln\left[C_n + P_{\text{Cl}}Z\right] + \frac{kT}{e}ln\left[P_{\text{K}}Z + C_d\right]
$$
$$
Z \equiv [\text{K}^+]_R = [\text{Cl}^-]_R \tag{4}
$$

If we are allowed to choose P_{Na}, P_{K} and P_{Cl} as is usually done, reproducing the data curve of Fig. 1 is not difficult. Assuming the following three equations, Eqs. 8 and 9 establish as long as Z is high enough.

$$
P_{\text{K}} \gg P_{\text{Na}} \tag{5}
$$

$$
P_{\text{K}}Z \gg C_d \tag{6}
$$

$$
P_{\text{Cl}} \sim 0 \tag{7}
$$

$$
C_n + P_{\text{Cl}}Z \sim C_n \tag{8}
$$

$$
P_{\text{K}}Z \gg C_d \tag{9}
$$

Using Eqs. 8 and 9, Eq. 4 can be approximated by Eq. 10. Equation 10 exhibits straight line with a slope of $+kT/e$. Therefore, the solid straight line in the higher ion concentration range in Fig. 1 is reproducible.

$$
\begin{aligned}
\phi(Z) &= -\frac{kT}{e}ln\left[C_n + P_{\text{Cl}}Z\right] + \frac{kT}{e}ln\left[P_{\text{K}}Z + C_d\right] \\
&\sim \frac{kT}{e}lnZ + \text{const.}
\end{aligned} \tag{10}
$$

When the ion concentration, Z, is lower, Eq. 8 still establishes and Eq. 11 establish.

$$
P_{\text{K}}Z + C_d \sim C_d \tag{11}
$$

Using Eqs. 8 and 11, Eq. 4 can be approximated by Eq. 12 and the last equation suggests that the potential change becomes indifferent to the change in ion concentration, Z, in the lower region of ion concentration, as indicated by the dashed line in Fig. 1.

$$
\begin{aligned}
\phi(Z) &= -\frac{kT}{e}ln\left[C_n + P_{\text{Cl}}Z\right] + \frac{kT}{e}ln\left[P_{\text{K}}Z + C_d\right] \\
&\sim +\frac{kT}{e}ln\left(\frac{C_d}{C_n}\right) = const.
\end{aligned} \tag{12}
$$

Therefore, the GHK eq. can reproduce all physiological potentials measured experimentally if one is allowed to determine the value of P_i at will. But can we rely on such values of P_i as an index showing the degree of membrane permeability to free ions? Shouldn't we refrain from using the GHK eq. so freely? The GHK eq. can reproduce the experimental membrane potentials, but it does not necessarily suggest that the membrane is ion permeable or that the membrane actually carries the same permeability coefficient as the estimated values.

The association-induction hypothesis interpretation

We mainly insist that the phenomenon of ionic adsorption cannot be neglected as a cause of membrane potential generation, and it is one of the main objectives of AIH (Ling 1992; Ling 1997; Ling 2001; Ling 2007). The AIH states that ion adsorption-desorption is governed by the law of mass action, and it leads to a heterogeneous three-dimensional ion distribution. Consequently, it results in a certain level of potential, which is called the membrane potential. Therefore, the membrane potential is generated as long as ion adsorption-desorption can take place, and the membrane permeability has almost nothing to do with the generation of the membrane potential according to the AIH.

Taking into account what is described in Sect. 2, we performed the experiments of membrane potential measurements and theoretical analyses described below (Fig. 2).

Experiment

The basic structure of the experimental setup we used for the membrane potential measurements in this work is illustrated in Fig. 3. The setup represents a cell, and both the left and right phases are the electrolytic solutions separated by an artificial membrane. The left phase and the right phase are filled with KCl (or LiCl) solutions and correspond to the cell-interior and the cell-exterior, respectively, and the (artificial) membrane corresponds to the plasma membrane. Then the membrane potential was measured.
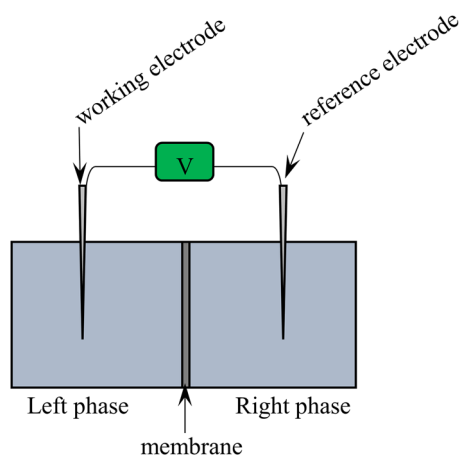
Fig. 2 The basic structure of setup employed to measure the potential difference across a membrane
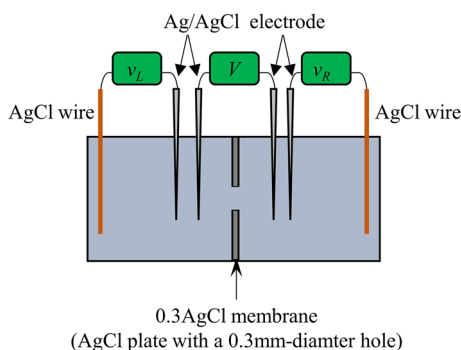

Fig. 3 Experimental setup with a 0.3AgCl membrane which has a 0.3-mm-diameter hole

KCl and LiCl solutions were prepared by the following procedure: A 1M KCl solution was prepared by dissolving KCl in deionized water. Then a 10^{-1}M KCl solution was prepared by diluting the 1M KCl solution by a factor of 10 with deionized water. In the same way, 10^{-2}M, 10^{-3}M, 10^{-4}M and 10^{-5}M KCl solutions were prepared. In the same manner, LiCl solutions ranging from 1 M–10^{-5}M were prepared.
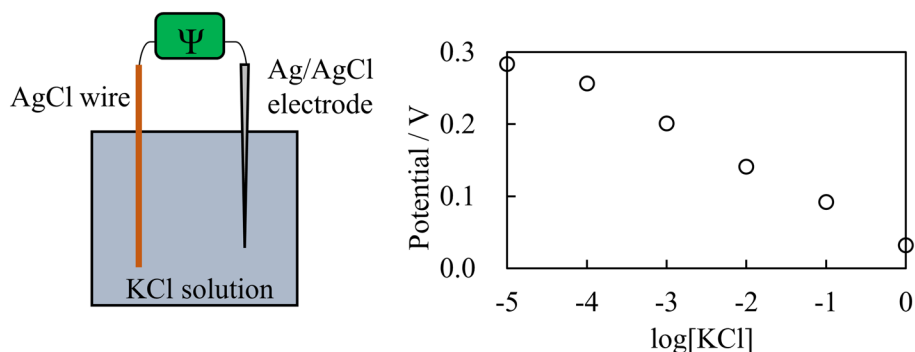
The actual experimental setup structures and the experimental conditions are detailed in Sect. 4.

Results and discussion

Potential across the solid permeable membrane

The experimental setup is shown in Fig. 3 and is detailed first. An AgCl plate with a hole (diameter = 0.3 mm) was fabricated by the following procedure: A 0.3-mm-diameter hole was created on a thin Ag plate. This plate was immersed in bleach for an hour, resulting in a plate coated with AgCl and will serve as a permeable membrane. We call it "0.3AgCl membrane" from now on. We also prepared two AgCl coated Ag wires by immersing two fine Ag wires in bleach for an hour. The resulting wire is to be called "AgCl wire". The left phase of the setup was filled with 10^{-4}M KCl solution, and right phase was filled with 1M KCl solution. Then the membrane potential, which is represented by "V" in Fig. 3 was measured as a function of time. Similarly, AgCl wire potentials in both left and right phases were also measured as a function of time. These potentials are represented by "v_L" and "v_R", respectively, as in Fig. 3. These wires were used to indirectly measure the ion concentration in the left and right phases as detailed in the following.

The AgCl wire exhibits a certain potential in relation to the Ag/AgCl electrode, and the potential is susceptible to the KCl concentration (Cheng 2002). There is a fairly clear one-to-one relationship between the potential and the concentration of the bathing KCl solution. Therefore, it is possible to estimate the concentration of the KCl solution by directly measuring the AgCl wire potential "Ψ". Figure 4 represents the potential of AgCl wire submerged in the KCl solutions. A clear one-to-one relationship exists between the potential and log[KCl]. Denoting -log[KCl] by x, Ψ is given by Eq. 13.

$$\Psi = -0.0025x^2 - 0.0642x + 0.03004 \tag{13}$$

Fig. 4 AgCl wire potential vs. concentration of KCl solution

Figure 5a shows the time dependence of the membrane potential generated across the 0.3AgCl membrane, which was measured using the setup shown in Fig. 3. Figure 5b shows the time dependence of KCl concentration in the left and right phases. Obviously, the membrane potential changes with time. The concentration of the left phase KCl increases with time and is undoubtedly caused by the diffusion of the right phase KCl into the left phase through the 0.3-mm-diameter hole of 0.3AgCl membrane. Since the concentration of the right phase KCl was originally quite high at 1M, the diffusion of KCl from the right phase to the left phase did not result in a visible change in the concentration of KCl in the right phase as seen in Fig. 5b.

It is quite natural to perceive that the change in membrane potential shown in Fig. 5a must be caused by the KCl diffusion across the 0.3 AgCl membrane. It is to be analysed using the GHK eq. Equation 14 is the GHK eq. for the potential profile shown in Fig. 5a.

$$\Psi = -\frac{kT}{e} \ln \frac{P_K[K^+]_L + P_{Cl}[Cl^-]_R}{P_K[K^+]_R + P_{Cl}[Cl^-]_R}$$

$[i]_j$: Concentration of i (i = K^+, Cl^-)

   in j phase (j = L(eft), R(ight))

(14)

Since the 0.3-mm-diameter hole of the 0.3AgCl plate does not have any function to selectively let the ions pass through, so no ion selectivity. Hence, $P_K = P_{Cl}$ is derived and Eq. 14 results in $\Psi \equiv 0$ at any time. However, the experimentally measured potential is nonzero (see Fig. 14a). There must be something to be amended about the GHK eq.

For comparison, we performed potential measurements on an impermeable plate AgCl using the setup illustrated in Fig. 3, where the AgCl plate without a hole was simply prepared by immersing a thin Ag plate without holes in bleach for an hour. The resulting AgCl plate is called a AgCl membrane. The measured potential across the AgCl membrane is shown in Fig. 6. The membrane potential is constant, and the ion concentration is constant. These are natural consequences. (This experiment was discontinued in the shorter period compared to Fig. 5 since no potential change and no change in ion concentration are expected, as intuitively understood.) Ion diffusion across the AgCl membrane never occurred. Hence, $P_K = P_{Cl} = 0$, and consequently results in the GHK eq. represented by Eq. 15, and it means the collapse of GHK eq. for this system. It could be argued that the GHK eq. should not be used when an impermeable separator is used. However, typically P_i's are not determined experimentally but rather are estimated, so
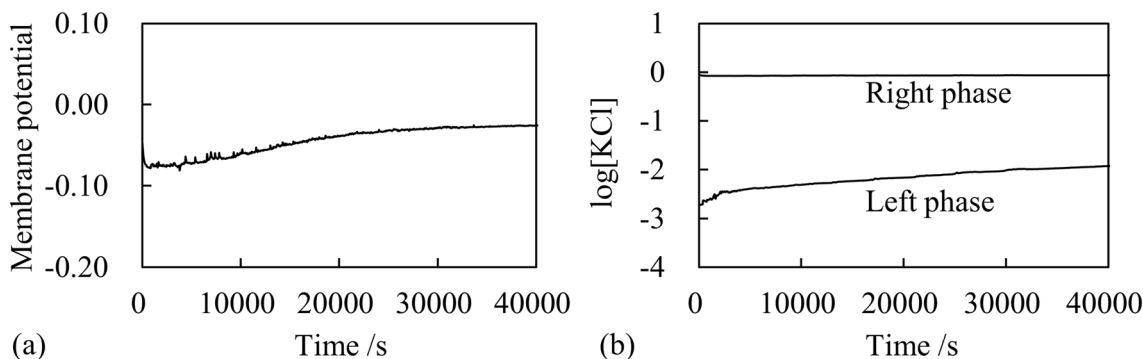

Fig. 5 **a** Membrane potential vs. Time; **b** *KCl* concentration vs. Time respect to *x* after plugging the experimentally measured v_L (v_R) into Ψ -log[*KCl*] of left (right) phase was obtained by solving Eq. 13 with

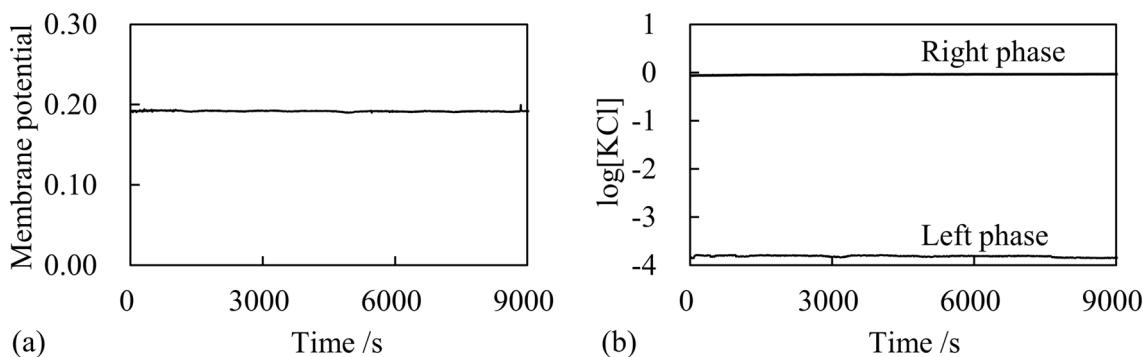**Fig. 6** **a** Membrane potential vs. Time; **b** KCl concentration vs. Time

that the GHK eq. reproduces the experimental membrane potentials without much considering the actual permeability of membranes (Tamagawa and Ikeda 2018; Wright and Diamond 1968; Olschewski et al. 2001; Uteshev 2010).

$$\Psi = -\frac{kT}{e} \ln \frac{P_K[K^+]_L + P_{Cl}[Cl^-]_R}{P_K[K^+]_R + P_{Cl}[Cl^-]_R}$$
$$= -\frac{kT}{e} \ln \frac{0 \cdot [K^+]_L + 0 \cdot [Cl^-]_R}{0 \cdot [K^+]_R + 0 \cdot [Cl^-]_R} = -\frac{kT}{e} \ln \frac{0}{0} \quad (15)$$

Therefore, whether AgCl membrane is permeable or not, the GHK eq. appears to be fundamentally incomplete if not wrong. Instead, our previous work suggests that the membrane potential is governed by the ion adsorption-desorption rather than the ion passage through the membrane. Therefore, we suggest that Eq. 2 is the most plausible equation for representing a membrane potential rather than the GHK eq. of Eq. 1.

Membrane potential under the AIH

AIH states that the ion adsorption-desorption process governs the generation of membrane potentials, while the membrane theory states that the flux of ions through the cell membrane governs it (Ling 1992; Ling 1997; Ling 2001, Ling 2007; Cronin 1987; Keener and Sneyd 2008; Ermentrout and Terman 2010). The AIH-based membrane potential formula is given by Eq. 2, where the derivation procedure of Eq. 2 is detailed in the ref. (Tamagawa and Ikeda 2018), and some of the derivation processes is to be touched upon in the Sect. 5 of this paper, too. This section explains the membrane potentials measured experimentally between two electrolyte solutions through the permeable and impermeable membranes. The experimental setup is the same as that shown in Fig. 3, but measurements of v_L and v_R were not made. Two types of membranes were used: One is an AgCl membrane (no holes) and another is a Li ion-conducting glass, LICGC™ AG-01 plate which was purchased from OHARA INC., (Kanagawa, Japan). From now on, the latter membrane will be called "Li membrane". According to the work done by Katoh et al. (Katoh et al. 2010), Li membrane is a permeable membrane. Then, we attempted to theorize those experimentally measured potentials from the point of view of the AIH.

Membrane potential across a AgCl membrane First, we measured the membrane potential across the AgCl membrane separating two KCl solutions. The KCl concentration in the right phase was maintained constant 10^{-4} M, while the KCl concentration in the left phase varied from 10^{-5} to 1 M. The experimental results are shown in Fig. 7. Although the AgCl membrane is impermeable, the GHK eq. can reproduce the experimental results using the hypothetical P_i as
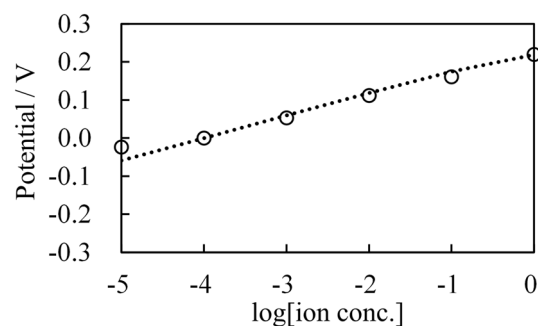

Fig. 7 Membrane potential across the AgCl membrane when the right phase solution = 10^{-4} M KCl   ∘ : Experimental, ⋯ : Theoretical (computed using Eq. 16)   Standard deviation of individual data is not shown here since it is invisibly small

shown in Eq. 16. However, such a theoretical analysis has no physiological significance since all P_i for this experimental system should be zero, and this means that the GHK eq. breaks down and has no scientific basis. However, P_i is usually estimated as that the GHK eq. can reproduce the experimental result by disregarding the actual membrane permeability to ions as touched upon in Sect. 1 (Tamagawa and Ikeda 2018; Wright and Diamond 1968; Olschewski et al. 2001; Uteshev 2010). It is a highly questionable scientific treatment.

$$V_{KCl}^{MP} = -\frac{kT}{e} ln \frac{P_K[K^+]_L + P_{Cl}[Cl^-]_R}{P_K[K^+]_R + P_{Cl}[Cl^-]_L} \quad (16)$$
$$P_K = 1 \quad P_{Cl} = 10000$$

On the other hand, AIH suggests that membrane potential arises from the spatial fixation of mobile ions at their adsorption sites (Ling 1992). Tamagawa and Ikeda performed the theoretical analysis based on physical chemistry. They suggested that the permeability coefficient P_i of the GHK eq. can be replaced by the association constant K_i between the mobile ion and the ion adsorption site (Tamagawa and Ikeda 2018). Regardless of the membrane permeability, the ion adsorption-desorption process based on the mass action law governs the membrane potential generation. It is detailed here in the following.

$$\phi = -\frac{kT}{e} ln \frac{K_K[K^+]_L + K_{Cl}[Cl^-]_R}{K_K[K^+]_R + K_{Cl}[Cl^-]_L} \quad (17)$$
K_i : the association constant between the mobile ion,

  i, and its adsorption site

Although the AIH is in total contradiction with the membrane theory, its scientific soundness has increased considerably in recent times (Chang 1983; Pollack 2013; Pollack 2014; Hwang et al. 2018; Kowacz and Pollack 2020;

Bagatolli and Stock 2021; Bagatolli et al. 2021; Schneider 2021; Wang and Pollack 2021; Wnek 2015; Jaeken 2017; Jaken 2021; Matveev 2019). The membrane potential in Fig. 7 is explainable using AIH here. First, we would like to analyse the slope of the data curve in Fig. 7, which is $\sim +kT/e$. Why is the slope $\sim +kT/e$? The AgCl membrane surface is AgCl. Therefore, adsorption of Cl^- to the membrane surface can take place (Temsamani and Cheng 2001). The AIH states that only the ions involved in the adsorption-desorption are involved in the potential generation. Since Cl^- adsorbs on the AgCl membrane surface and K^+ does not, $K_{Cl} \neq 0$ and $K_K = 0$ are derived. Hence, Eq. 17 is transformed into Eq. 18, and it suggests that the slope of the potential curve is $\sim +kT/e$. Then, Eq. 18 can reproduce the virtually straight-line membrane potential profile in Fig. 7.

$$\begin{aligned} \phi &= -\frac{kT}{e} ln \frac{K_K[K^+]_L + K_{Cl}[Cl^-]_R}{K_K[K^+]_R + K_{Cl}[Cl^-]_L} \\ &\sim -\frac{kT}{e} ln \frac{K_{Cl}[Cl^-]_R}{K_{Cl}[Cl^-]_L} = +\frac{kT}{e} ln \frac{[Cl^-]_L}{[Cl^-]_R} \end{aligned} \tag{18}$$

We will analyse in more detail the membrane potential behaviour. The dotted lines in Fig. 8 represent the expected potential profiles. It has been experimentally confirmed that the surface potential of the membrane *AgCl* submerged in deionized water is around 0.3 V compared to the bulk phase potential of deionized water (Tamagawa and Ikeda 2018; Tamagawa 2018). But once the Cl^- concentration of the bathing solution increases, the Cl^- adsorption on the AgCl surface increases, causing the decrease of AgCl surface potential due to the negative charge of adsorbed Cl^-. Since the amount of Cl^- adsorbed on the AgCl membrane right surface is greater than that of AgCl membrane left surface, $|V_L| > |V_R|$ is derived as in Fig. 8. AIH suggests that potential profiles in the left phase and right phase are
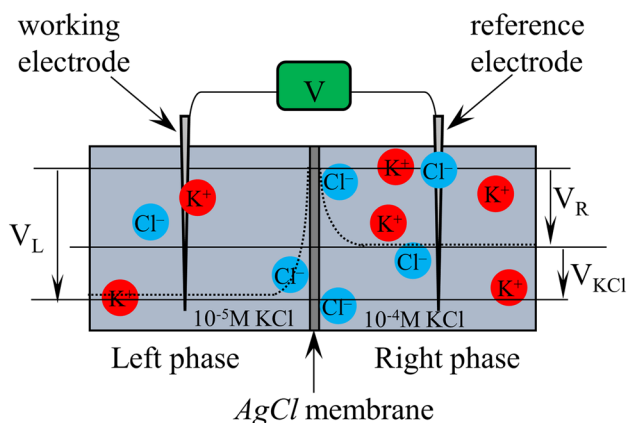

Fig. 8 Ion adsorption and expected potential profiles (Dotted curves) If the membrane surface potential is defined as zero, V_L and V_R are negative

determined independently of each other. Therefore, the membrane potential is given simply by Eq. 19.

$$V_{KCl} = V_L - V_R \tag{19}$$

According to Eq. 19, membrane potential shown in Fig. 7 (denoted by V_{KCl}^{MP}) can be mathematically represented by Eq. 20. That is, $V_{KCl}^{MP} (= V_{KCl}^{MP}(C_L, C_R))$ is merely the difference between two potentials $V_L (= V_L(C_L))$ and $V_R (= V_R(C_R))$ which were independently determined mutually, and $V(C_R)$ remains constant throughout the measurement since C_R is maintained 10^{-4}M. Therefore, $V_{KCl}^{MP}(C_L)$ is a function of C_L only.

$$V_{KCl}^{MP}(C_L, C_R) = V_L(C_L) - V_R(C_R), \quad C_R = 10^{-4}M$$
C_L, C_R : the KCl concentration of Left phase, of Right phase
$$\tag{20}$$

The same membrane potential measurement was performed by using 10^{-2} M KCl solution as the right phase in place of 10^{-4} M KCl solution. As long as the cause of membrane potential generation is attributed to the ion adsorption-desorption as AIH states, the same discussion above is available and the measured membrane potential, $V_{KCl}^{MP}(C_L')$, can be given by Eq. 21, and of course $V_R(C_R' = 10^{-2}M)$ maintained constant throughout the measurement.

$$V_{KCl}^{MP}(C_L', C_R') = V_L(C_L') - V_R(C_R'), \quad C_R' = 10^{-2}M$$
C_L', C_R' : the KCl concentration of Left phase, of Right phase
$$\tag{21}$$

In the context of this discussion based on the ion adsorption-desorption phenomenon, $V(C_L) = V(C_L')$ establishes when $C_L = C_L'$. The potential difference between $V_{KCl}^{MP}(C_L, C_R = 10^{-4}M)$ and $V_{KCl}^{MP}(C_L', C_R' = 10^{-2}M)$ is given by Eq. 22 as ΔV_{KCl}^{MP}, and it is constant as long as $C_L = C_L'$ as given by Eq. 23.

$$\begin{aligned} \Delta V_{KCl}^{MP} &= V_{KCl}^{MP}(C_L, 10^{-4}M) - V_{KCl}^{MP}(C_L', 10^{-2}M) \\ &= \left[V_L(C_L) - V_R(C_R = 10^{-4}M) \right] - \left[V_L(C_L') - V_R(C_R' = 10^{-2}M) \right] \end{aligned} \tag{22}$$

$$= -V_R(10^{-4}M) + V_R(10^{-2}M)) = const. \tag{23}$$

Therefore, the potential data curve of $V_{KCl}^{MP}(C_L, C_R = 10^{-4}M)$ vs. $log[C_L]$ must be parallel to that of $V_{KCl}^{MP}(C_L', C_R' = 10^{-2}M)$ vs. $log[C_L']$. In fact, they are in the parallel relationship as in Fig. 9a. It validates the AIH. But GHK eq. of Eq. 16 also reproduces the experimental potential data as represented by the straight dotted and dashed lines in Fig. 9b, although physically meaningless P_i's are in use. Equation 16 can be transformed as shown by Eq. 24. The last term is identical to the Nernst equation. Nernst equation results in straight lines in Fig. 9b.
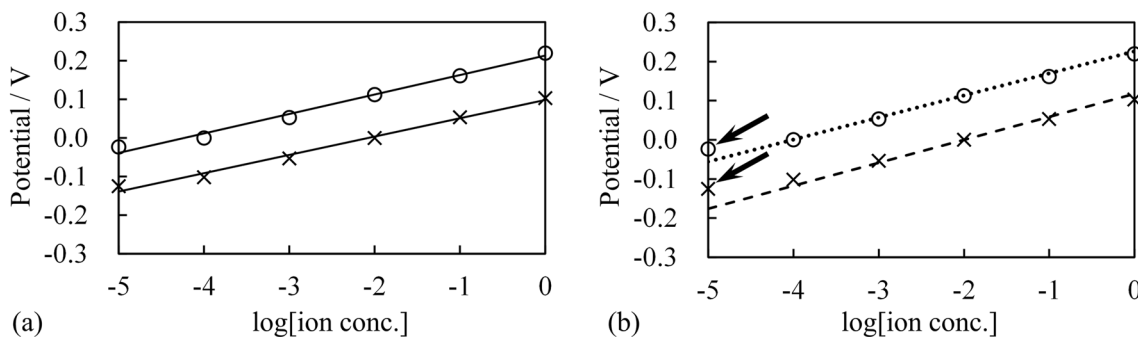
Fig. 9 Membrane potential across the AgCl membrane (**a**) Experimental data of $V_{KCl}^{MP}(C_L)$ vs. $\log[C_L]$ when $[C_L] = 10^{-4}$ M (○) and its linear trend line obtained by the least square method (—), Experimental data of $V_{KCl}^{MP}(C_L')$ vs. $\log[C_L']$ when $[C_L'] = 10^{-2}$ M (×) and its linear trend line obtained by the least square method (—) **b** Experimental data of $V_{KCl}^{MP}(C_L)$ vs. $\log[C_L]$ when $[C_L] = 10^{-4}$ M (○) and the theoretical linear line obtained by Eq. 16 (…), Experimental data of $V_{KCl}^{MP}(C_L')$ vs. $\log[C_L']$ when $[C_L'] = 10^{-2}$ M (×) and the theoretical linear line obtained by Eq. 16 (- - -) Standard deviation of individual experimental data is not shown here since it is invisibly small

$$V_{KCl}^{MP} = -\frac{kT}{e} ln \frac{P_K[K^+]_L + P_{Cl}[Cl^-]_R}{P_K[K^+]_R + P_{Cl}[Cl^-]_L} \sim -\frac{kT}{e} ln \frac{P_{Cl}[Cl^-]_R}{P_{Cl}[Cl^-]_L}$$
$$= -\frac{kT}{e} ln \frac{[Cl^-]_R}{[Cl^-]_L}$$

(24)

Membrane potential across a Li membrane The same experiments for obtaining the diagrams in Fig. 9 were performed using the Li membrane in place of the AgCl membrane and using LiCl solutions in place of KCl solutions. The results are shown in Fig. 10 together with the theoretical results obtained using Eq. 25. The parallel experimental data validates the AIH, but GHK eq. of Eq. 26 can reproduce the experimental potential data. It is explained in detail as follows.

$$V_{LiCl}^{MP} = -\frac{kT}{e} ln \frac{P_{Li}[Li^+]_L + P_{Cl}[Cl^-]_R}{P_{Li}[Li^+]_R + P_{Cl}[Cl^-]_L}$$
$$P_{Li} = 1000, \ P_{Cl} = 1$$

(25)

According to the specification of Li membrane (Li conducting glass plate) and the report by Katoh et al. (Katoh et al. 2010), Li membrane is permeable only to Li$^+$. Hence, it appears to be possible for us to believe $P_{Li} \gg P_{Cl}$ without any violation of the law of physics. Hence, Eq. 25 can be approximated by Eq. 26. The last term is identical to the Nernst eq. (just like Eq. 24). Nernst eq. results in the straight lines in Fig. 10b.
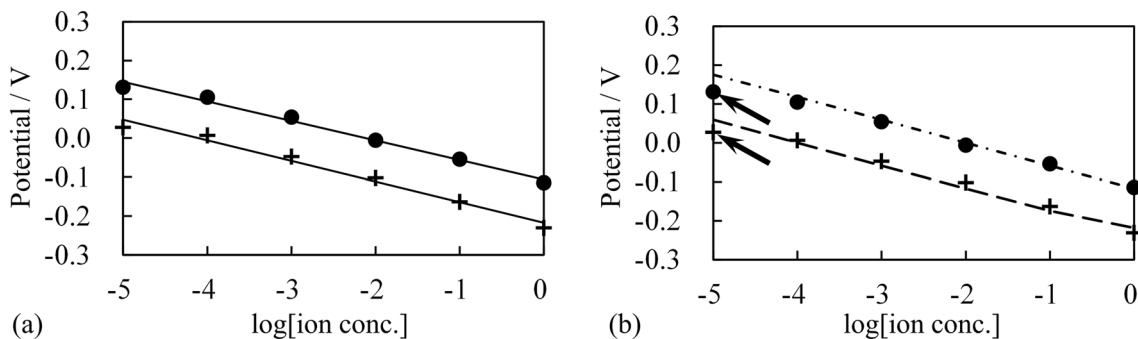

Fig. 10 Membrane potential across the AgCl membrane **a** Experimental data of $V_{LiCl}^{MP}(C_L)$ vs. $\log[C_L]$ when $[C_L] = 10^{-4}$ M (•) and its linear trend line obtained by the least square method (—), Experimental data of $V_{LiCl}^{MP}(C_L')$ vs. $\log[C_L']$ when $[C_L'] = 10^{-2}$ M (+) and its linear trend line obtained by the least square method (—) **b** Experimental data of $V_{LiCl}^{MP}(C_L)$ vs. $\log[C_L]$ when $[C_L] = 10^{-4}$ M (•) and the theoretical linear line obtained by Eq. 25 (- · - · -), Experimental data of $V_{LiCl}^{MP}(C_L')$ vs. $\log[C_L']$ when $[C_L'] = 10^{-2}$ M (+) and the theoretical linear line obtained by Eq. 25 (– – –) Standard deviation of individual experimental data is not shown here since it is invisibly small

$$
\begin{aligned}
V_{\text{LiCl}}^{\text{MP}} &= -\frac{kT}{e} ln \frac{P_{\text{Li}}[\text{Li}^+]_L + P_{\text{Cl}}[\text{Cl}^-]_R}{P_{\text{Li}}[\text{Li}^+]_R + P_{\text{Cl}}[\text{Cl}^-]_L} \sim -\frac{kT}{e} ln \frac{P_{\text{Li}}[\text{Li}^+]_L}{P_{\text{Li}}[\text{Li}^+]_R} \\
&= -\frac{kT}{e} ln \frac{[\text{Li}^+]_L}{[\text{Li}^+]_R}
\end{aligned}
\tag{26}
$$

The use of Eq. 26 can quantitatively predict the experimental membrane potential shown in Fig. 10b. Therefore, there appears to be nothing wrong with the membrane theory. However, how can we justify Eq. 16 physically? P_i of Eq. 16 should be zero, and it collapses Eq. 16. As we say repeatedly, P_i of Fig. 16 is physically wrong, while mathematically valid. Now we would like to discuss the following two intriguing points.

1. The GHK eq. of Eq. 16 can be approximated by Eq. 24 by employing P_i's (given in Eq. 16 as well). Equation 24 can quantitatively predict the experimental membrane potential shown in Fig. 9. Similarly, the GHK eq. of Eq. 26 perfectly reproduces the experimental membrane potentials in Fig. 10. However, Eq. 16 and its approximation Eq. 24 are both originally wrong since their P_i's should be zero. However, the use of hypothetical nonzero P_i's reproduces the experimental results in Eq. 16. Even more intriguingly, Eq. 24 is a function of the anion concentration, while Eq. 26 is a function of the concentration of ions. These two equations are symmetric about the sign of an ion, and both can reproduce the experimental results. It makes us envision that there must be some common mechanism of membrane potential generation for both systems for Figs. 9 and 10, though Eq. 16 and its approximation Eq. 24 both appear to be originally wrong, as mentioned above. The previous work by Tamagawa and Ikeda could answer such a query. Their work suggested that the GHK eq. (Eq. 16) can be reinterpreted as Eq. 17 using the AIH (Tamagawa and Ikeda 2018). K_i in Eq. 17 is a binding constant between the mobile ions and the adsorption sites. The silver oxide of the AgCl membrane must serve as Cl^- adsorption sites (Temsamani and Cheng 2001), $K_K = 0$ and $K_{\text{Cl}} = \text{nonzero}$ are naturally derived. Hence, Eq. 27 is derived.

$$
\begin{aligned}
V_{\text{KCl}}^{\text{MP}} &= -\frac{kT}{e} ln \frac{K_K[\text{K}^+]_L + K_{\text{Cl}}[\text{Cl}^-]_R}{K_K[\text{K}^+]_R + K_{\text{Cl}}[\text{Cl}^-]_L} \\
&= -\frac{kT}{e} ln \frac{K_{\text{Cl}}[\text{Cl}^-]_R}{K_{\text{Cl}}[\text{Cl}^-]_L} = -\frac{kT}{e} ln \frac{[\text{Cl}^-]_R}{[\text{Cl}^-]_L}
\end{aligned}
\tag{27}
$$

Similarly, assuming the Li membrane serves as Li^+ adsorption sites, $K_{\text{Li}} = \text{nonzero}$ and $K_{\text{Cl}} = 0$ are easily derived. Hence, Eq. 28 is derived.

$$
\begin{aligned}
V_{\text{LiCl}}^{\text{MP}} &= -\frac{kT}{e} ln \frac{K_{\text{Li}}[\text{Li}^+]_L + K_{\text{Cl}}[\text{Cl}^-]_R}{K_{\text{Li}}[\text{Li}^+]_R + K_{\text{Cl}}[\text{Cl}^-]_L} \\
&= -\frac{kT}{e} ln \frac{K_{\text{Li}}[\text{Li}^+]_L}{K_{\text{Li}}[\text{Li}^+]_R} = -\frac{kT}{e} ln \frac{[\text{Li}^+]_L}{[\text{Li}^-]_R}
\end{aligned}
\tag{28}
$$

These two equations are symmetric in terms of the sign of ion charge. On top of that, the last terms of Eqs. 27 and 28 are identical to the Nernst equation. Further analysis suggests that the absolute experimental membrane potential shown in Fig. 10 is even quantitatively the same as those in Fig. 9. So, the membrane potentials in Fig. 10 and those in Fig. 9 are symmetric about the x-axis even quantitatively. The AIH-based equations for potentials, Eqs. 27 and 28, provide the symmetric potential profile of the horizontal axis when $V_{\text{salt}}^{\text{MP}}$ vs. $\log_{10}[(\text{salt})_L]$ is considered.

2. All membrane potentials in the lowest ion concentration region, which are indicated by arrows in Figs. 9b and 10b, deviate from the theoretical straight membrane potential lines predicted using the GHK equation. Namely, the change in membrane potential becomes indifferent to the change in ion concentration in the lowest ion concentration milieu. Such a deviation of the membrane potential from the straight line (Nernst equation type) has often been observed in the region of very low ion concentrations (Tamagawa et al. 2021b; Hodgkin and Howrowicz 1959; Diamond and Harrison 1966; Shinagawa 1976; Chang 1983; Zhang and Wakamatsu 2002). As stated in the Sect. 2.1 employing Fig. 1, such a membrane potential behaviour is easily explained by the GHK eq. if any numerical value is allowed to use as P_i. But such P_i does not have any physiological meaning. On the other hand, the ion adsorption-desorption mechanism based on AIH can explain this reaction without any unusual assumption. Firstly, see Fig. 8 and assume that the KCl concentration in the left phase is quite low. Due to the relatively low concentration of KCl, the quantity of Cl^- on the left surface of the membrane must be quite small. The further decrease in KCl concentration in the left phase must be unable to cause a further decrease in the amount of adsorbed Cl^- since the quantity of adsorbed Cl^- is quite small at first. Therefore, the change in membrane potential becomes indifferent to the ion concentration change at the lowest ion concentration milieu.

The two above points are explainable by attributing membrane potential generation to the ion adsorption suggested by AIH.

Membrane potential across the combinatorial membrane From what has been described so far, it is not unreasonable to assume that V_L and V_R are governed by ionic adsorption
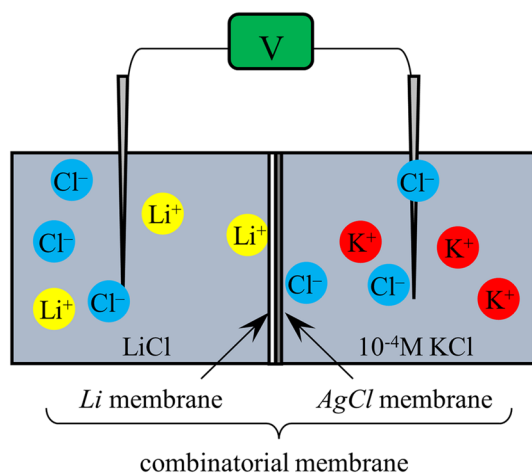
Fig. 11 Membrane potential across the combinatorial membrane consisting of a Li membrane and an AgCl membrane   The Li membrane is in contact with the left phase solution, while the AgCl membrane is in contact with the right phase solution

Fig. 12 •, +: The membrane potentials shown in Fig. 10a along with their straight trend lines   △: The membrane potential across the combinatorial membrane (see Fig. 11) and its dotted straight trend line   Standard deviation of potential represented by △ is shown here only, since the others are invisibly small.   All the trend lines were obtained by the least square method

independently of each other and that the membrane potential is simply the difference between V_L and V_R. We made measurements using the setup illustrated in Fig. 11. The left phase is filled with a LiCl solution, while the right phase is filled with a 10^{-4} M KCl solution. The membrane used is a combination of a Li membrane and a AgCl membrane. The Li membrane is in contact with the left phase LiCl solution, while the AgCl membrane is in contact with the right phase KCl solution. The membrane potential across this combinatorial membrane was measured by varying the concentration of the left phase LiCl from 10^{-5} to 1 M along with maintaining the right phase KCl concentration at 10^{-4} M. The variation of LiCl concentration must result in the experimental membrane potential graph parallel to the graphs shown in Fig. 10, and the membrane potential at [LiCl] = 10^{-5} M is expected to deviate from the straight trend line of the membrane potential data. Figure 12 shows the experimental membrane potential here obtained (△) and its straight trend line (…) along with the data shown in Fig. 10a, where the horizontal axis represents the logarithm of $[LiCl]_L$. The parallel relationship and the data deviation indicated by an arrow are observed. This result is in line with the AIH prediction and can justify the AIH, while it is inexplicable by the membrane theory due to the impermeable property of the combinatorial membrane (the membrane part AgCl is obviously impermeable).

Potential across the liquid permeable membrane

We found in Sect. 4.2 that the "Potential vs. log[ion conc.]" profiles exhibit a parallel relationship one another as long as the left solution is used and the left surface characteristics of the membrane are unchanged. In order to see the universality
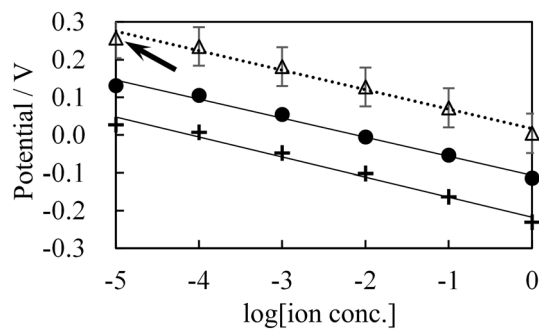
of such phenomena, we performed the same experiment: We made measurements of potential across the liquid membrane instead of the solid membrane. It is more like a living cell.

We prepared four types of electrolytic sols and used them as liquid membrane. Figure 13 illustrates the actual experimental setup and the four types of liquid membranes which are indicated by C-sol, A-sol, CA-sol and AC-sol, respectively. C-sol is a cationic sol, while A-sol is an anionic sol. CA-sol and AC-sol consist of both the C-sol and A-sol but the position arrangement of the C-sol and A-sol is opposite to each other.

These sols were prepared by the following procedure: To 50 ml of deionized water, monomers, polymerization accelerator (N,N,N',N'tetramethylethyldiamine, 0.005g) and polymerization initiator (ammonium persulfate, 0.04 g) were added in a systematic and homogeneous manner where the monomers used for the synthesis of C-sol and A-sol were "acrylamide (4.26g) and allylaminehydrochloride (1.80g)" and "acrylamide (4.26g) and acrylic acid (1.44g)", respectively. The resulting mixture was heated in 65 °C water bath for one hour. After completion of the sol synthesis, a large quantity of ethanol was mixed with the sol. The sol was precipitated, retrieved, and mixed again with deionized water. Ethanol was added, resulting in precipitated sol. By this ethanol/deionized water solvent exchange, the sol was washed. Then the sol was fully dried in the oven. This fully dried sol was mixed with deionized water in a weight ratio of 1:4.

The membrane potential across the C-sol and CA-sol was measured by varying the left phase KCl concentration while maintaining the right phase KCl concentration at 10^{-4} M. The left phase KCl solutions are in contact with C-sol whichever C-sol or CA-sol is used. Hence, the expected membrane potential generated across the C-sol must be different from that across the CA-sol by a constant value as long as the concentration of left phase KCl in contact with

Fig. 13 Experimental setup for measuring the membrane potential across the liquid membranes denoted by C-sol, A-sol, CA-so and AC-sol. The checkered pattern represents the dialysis membrane used to prevent the flow of sol
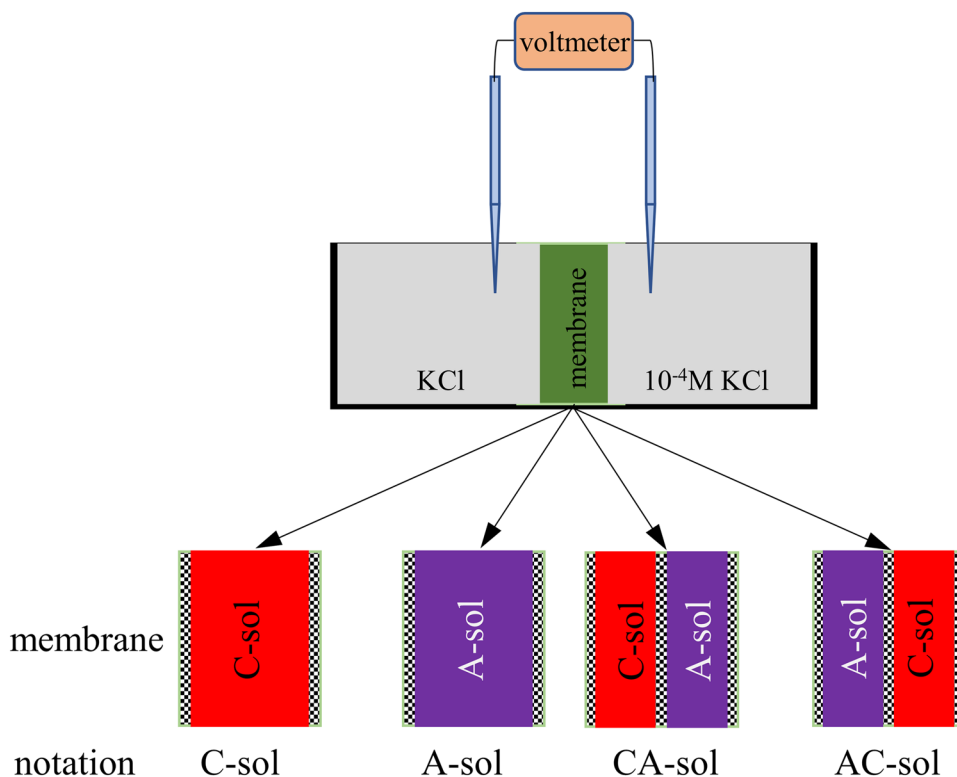
the C-sol is the same as that in contact with the CA-sol, as clearly understood by the discussion in the Sect. 4.2. Figure 14(a) shows "the membrane potential vs. log [KCl] in the left phase" and their trend lines. As expected, the difference between the membrane potentials across the C-sol and the CA-sol is almost constant, even though the KCl concentration varies by more than the factor of thousands. Figure 14b shows the membrane potential profiles in the A-sol and the AC-sol. The difference between the membrane potentials is, as expected, almost constant regardless of the ion concentration.

Membrane potential characteristics and formula

One of the authors of this article (H.T.) derived a formula of membrane potential in the ref. (Tamagawa and Ikeda 2018). We again scrutinize the computational results described in the ref. (Tamagawa and Ikeda 2018) and discuss the fundamental facet of membrane potential profiles, especially typified by the parallel potential profiles shown in Sect. 4.2. First, we introduce the summary of the essential part of the ref. (Tamagawa and Ikeda 2018) as below.
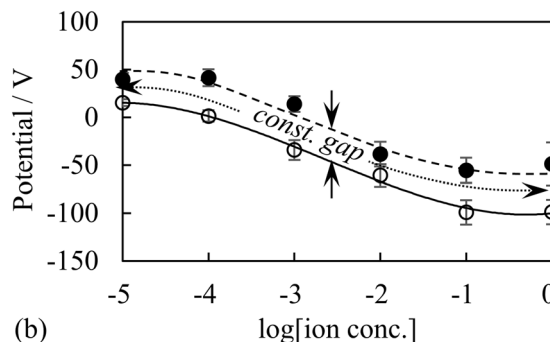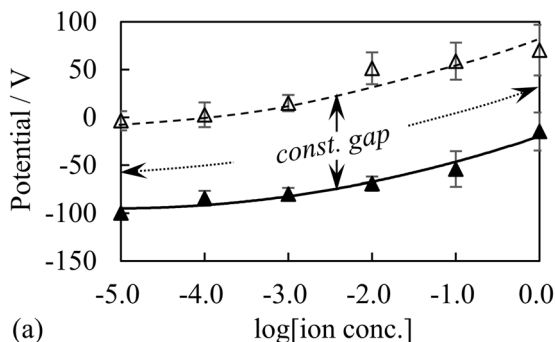

Fig. 14 Membrane potential across the sol vs. log[KCl] in the left phase **a** membrane potential across the C-sol ($\triangle$) and the CA-sol ($\blacktriangle$) and their trend lines (a solid and a dashed lines) The gap between the two trend lines is virtually constant. **b** membrane potential across A-sol ($\bigcirc$) and AC-sol ($\bullet$) and its trend links (a solid and a dashed lines) The gap between the two trend lines is virtually constant

Tamagawa and Ikeda measured the potential generated between two electrolytic solutions, both of which consist of KCl and KBr. These two solutions were electrically connected by an Ag wire coated with AgCl. Assuming that the membrane potential obeys AIH and that Cl^- and Br^- are prone to be adsorbed on the surface of AgCl, the surface charge density of AgCl surface of Ag wire ($\sigma|_{x=0}$) was calculated and found that the surface charge density was kept almost constant unless the electrolytic solution ion concentration was extremely high or extremely low. The actual formula from which they derived is given by Eq. 29, where the definitions of individual physical quantities in Eq. 29 are given in the ref. (Tamagawa and Ikeda 2018).

$$\sigma|_{x=0} = 2\sqrt{2\epsilon\epsilon_0 Q_0 kT} \sinh(e\phi|_{x=0}/kT)$$
$$= \sigma_0 - e[s]_T \frac{(K_{Cl}Q_{Cl} + K_{Br}Q_{Br})\exp(e\phi|_{x=0}/kT)}{1 + (K_{Cl}Q_{Cl} + K_{Br}Q_{Br})\exp(e\phi|_{x=0}/kT)} \quad (29)$$

As long as the ion concentration of the electrolytic solution was moderate - greater than 10^{-5} M but less than 1M -, the computationally obtained $\sigma|_{x=0}$ was found to be constant. Therefore, Eq. 29 was arranged into Eq. 30.

$$\text{const.} \sim \sigma|_{x=0} = \frac{\sigma_0}{1 + (K_{Cl}Q_{Cl} + K_{Br}Q_{Br})\exp(e\phi|_{x=0}/kT)} \quad (30)$$

Solving Eq. 30 with respect to $\phi|_{x=0}$ resulted in Eq. 31.

$$\phi|_{x=0} = \frac{kT}{e} \ln \frac{A}{K_{Cl}Q_{Cl} + K_{Br}Q_{Br}}, \quad A \equiv const. \quad (31)$$

Essential part of what Eq. 30 suggests is simplified and explained by Fig. 15. The surface charge density is virtually constant as long as the ion concentration is moderate. However, the screening in accordance with the ion concentration determines the potential profiles in the left and right solutions independently of each other.

As clearly seen in Fig. 15, the membrane potential, Φ, is given by Eq. 32. Plugging Eq. 31 into Eq. 32 results in Eq, 33, and it can be further arranged into Eq. 34. Equation 34 is identical to the GHK eq., but its physiological meaning is completely different from the GHK eq. Equation 34 is derived on the premise that the membrane potential is governed by the ion adsorption, as clearly understood by the fact that Eq. 34 contains the binding constant K_i.

$$\Phi = -\phi|_{x=0}^L - (-\phi|_{x=0}^R) \quad (32)$$

$$= -\frac{kT}{e} \ln \frac{A}{K_{Cl}Q_{Cl}^L + K_{Br}Q_{Br}^L} - \left(-\frac{kT}{e} \ln \frac{A}{K_{Cl}Q_{Cl}^R + K_{Br}Q_{Br}^R}\right) \quad (33)$$
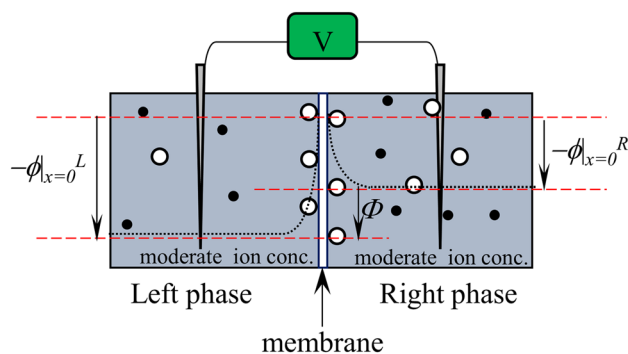

Fig. 15 A membrane intervenes between two electrolytic solutions (ions are represented by ○ and •) The concentrations of two electrolytic solutions are moderate. Regardless of the concentration of ions, the quantity of ions adorbed on the surface of the left membrane is the same as that on the surface of the right membrane. Consequently, the membrane left surface charge density is the same as the right surface charge density

$$= -\frac{kT}{e} \ln \frac{K_{Cl}Q_{Cl}^R + K_{Br}Q_{Br}^R}{K_{Cl}Q_{Cl}^L + K_{Br}Q_{Br}^L} \quad (34)$$

To reach Eq. 34, Eq. 31 is the key equation. But the theoretical treatment requires the use of ion adsorption. In the chemical, biological, and physiological process, the ion adsorption is inevitable. No chemical, biological and physiological processes are responsible for the absence of ion adsorption (or association). Therefore, it is not unnatural to speculate that the ion adsorption-desorption process is involved in the membrane potential generation process. In view of thermodynamics, ion characteristics should be viewed as thermodynamically real rather than ideal ones. In fact, such a thermodynamic treatment was proposed decades ago even in the biological and physiological studies (Ling 1992; Ling 2001; Lewis and Randall 1961).

Physiological activity and physics and physical chemistry

Some example of potential generation by ion adsorption

Our work suggests that the generation of membrane potential must be caused by the ion adsorption-desorption of ions rather than by the transmembrane ion transport. But such a mechanism of potential generation is not really new in a research field other than physiology. A typical example is the ion-selective electrode (ISE). The ISE can detect a particular ionic species dissolved in solution. Although it is not appropriate to say that the ISE working mechanism is fully elucidated, researchers must agree that adsorption of

ions onto the ISE selective membrane could explain its functionality (Cheng 1998; Cheng 2002; Covington 1981; Durst 1969; Rechnitz 1973; Fischer 1974; Radu et al. 2013; Naik 2016; Berg 2021; Criscuolo et al. 2021). Above all, Cheng's emphasis on the ISE mechanism is quite intriguing. Cheng suggests that the entire function of ISE is attributed to the adsorption of analyte ions on the surface of the ISE membrane (Tamagawa et al. 2021b; Cheng 1998; Cheng 2002). That is, the ISE potential depends on the affinity of the analyte ion to the ISE membrane. Therefore, the ISE can detect the concentration of a particular ionic species in the solution as an electrical signal. This mechanism is in harmony with physical chemistry and physics. Up until today, there have been countless reports on ISE mechanisms whether all ISE functionality mechanisms can be attributed to ion adsorption or not (Cheng 1998; Cheng 2002; Covington 1981; Durst 1969; Rechnitz 1973; Fischer 1974; Radu et al. 2013; Naik 2016; Berg 2021; Criscuolo et al. 2021). The potential generation by the ion adsorption is a fairly commonly accepted notion in the ISE research field. Ion adsorption is a thermodynamically treatable phenomenon. In fact, thermodynamic analysis of ion adsorption has been one of the primary topics in physical chemistry. Thermodynamics never distinguishes non-living systems from living systems. Therefore, the thermodynamics which is right in a certain research field such as the ISE research is also right in physiology. However, such an intimate correlation between the potential generation and the ion adsorption is completely ignored in current physiology.

Is it possible to explain the potential profile in Figs. 5a and 6a by the AIH? Yes, it is possible as below. Figure 16 represents the state of the ions adsorbed on the membranes. Ion adsorption inevitably takes place according to the mass action law whether or not the membrane is permeable (Tamagawa and Ikeda 2018; Tamagawa 2018; Barrow 1979). According to the discussion described in Sect. 5, the quantities of ions adsorbed on the left and right surfaces of the membrane are basically the same as each other regardless of the concentration of the solution ions. However, the degree of screening depends on the ion concentration, and it determines the potentials in the left and right solutions independently of each other. Therefore, the potential profile in the left solution can be different from that in the right solution. Therefore, various nonzero membrane potentials can be generated regardless of the membrane permeability to ions. The ion adsorption-desorption is a quite plausible cause of membrane potential generation (Ling 1992; Ling 1997; Ling 2001; Ling 2007).

Interfacial charge distribution

One author, Tamagawa, reported that the GHK eq., for example, Eq. 1, should be rewritten by Eq. 2 (Tamagawa and Ikeda 2018). If K^+ and Cl^- account for all mobile ions in the system in question, Eq. 2 can be written in Eq. 17. With this equation in mind, we consider the potential profile generated across a permeable membrane. Imagine a system consisting of two electrolytic solutions separated by a permeable membrane illustrated in Fig. 17. If a nonzero membrane potential is generated, a heterogeneous spatial mobile ion distribution should occur. However, mobile ions in the bulk phase cannot distribute autonomously in a heterogeneous way. How does the heterogeneous ion distribution take place?

Heterogeneously structured biological environments such as the interface between the plasma membrane and the protoplasm of living cells can serve as heterogeneously distributing adsorption sites for mobile ions regardless of the membrane permeability and can lead to the heterogeneous ion distribution. It is illustrated more clearly in Fig. 17. Local positive (nonzero) charges are generated on the membrane surface. Although the microscopic electroneutrality is violated at the interface between the left solution and the membrane encircled by the dashed line (it is true at the interface between the right phase solution and the membrane as well), the macroscopic electroneutrality is sufficient in the entire left phase circled by the dotted line (it is true for the

Fig. 16 **a** experimental setup employing a permeable membrane **b** experimental setup employing an impermeable membrane ○: ions adsorbed on the membrane surface
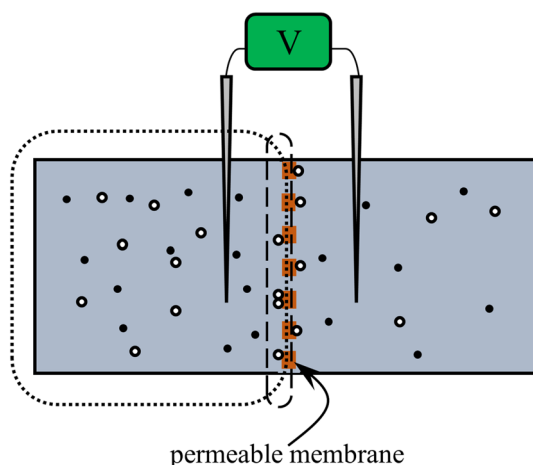
(a) permeable membrane   (b) impermeable membrane
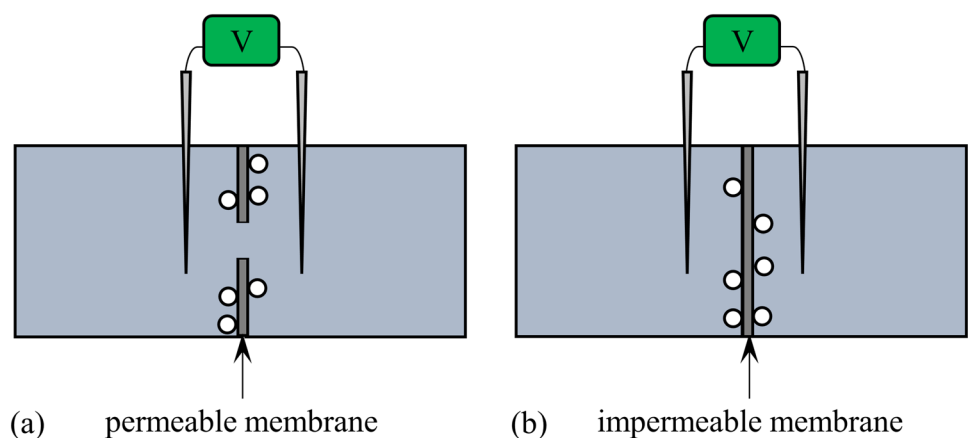
Fig. 17 Two electrolytic solutions separated by a permeable membrane where the left phase ion concentration is greater than that in the right phase ○ mobile ion, • mobile counter ion

Fig. 18 Potential profile of anionic hydrogel (containing immobile negative charges) submerged in an electrolytic solution ○ : anion, • : cation dashed line: potential profile

entire right phase). The violation of microscopic electroneutrality can be fully allowed thermodynamically and can lead to nonzero potential generation. A capacitor is a typical example: The total sum of charges the capacitor holds is zero, while the positive and negative charges exist separately from each other in the capacitor in microscopic view. As immediately and intuitively understood by considering the functionality of a capacitor, the localized charge distribution illustrated in Fig. 17 inevitably leads to the generation of nonzero potential. Such a nonzero potential must be the membrane potential. It has nothing to do with the membrane permeability. So, the localized charge generates the nonzero potential as predicted by electromagnetism; that is all. Isn't it rational to believe the membrane potential is generated by such a mechanism that is in line with basic physics, thermodynamics and electromagnetism? Given that the membrane potential is generated by the transmembrane ion transport, as predicted by membrane theory, how is the influence of the plasma membrane surface charges on the membrane potential nullified? Is physiology in conflict with thermodynamics and electromagnetism? Something important is missing from membrane theory. Membrane theory should be at least amended, if not wrong.

We can speculate that the generation of nonzero membrane potentials may not take advantage of the selective permeability of the plasma membrane. We measured the potential of meat sold in an ordinary supermarket. The cell of this meat has a plasma membrane, but the sodium pump embedded in it does not function because the cells of the sold meat are dead cells. However, we observed that the meat submerged in the electrolytic solution exhibited a nonzero potential. Therefore, we raise the question of whether the sodium pump is truly needed for the
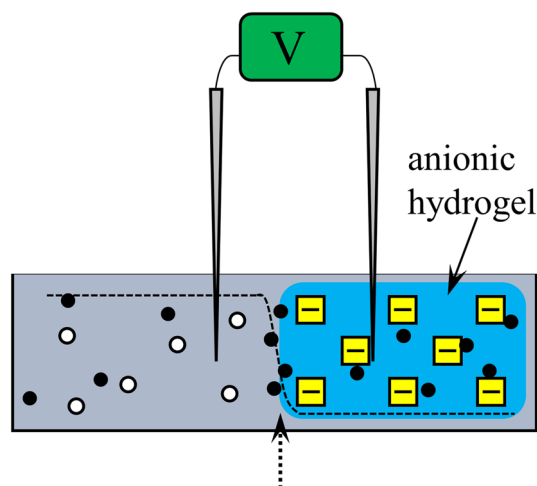
generation of membrane potential. Sodium pumps and ion channels may not be needed to explain the generation of membrane potential. But how was the nonzero potential generated without a membrane? This could be attributed to the ion adsorption at the interface. Pollack's reports are typical examples. Pollack and his associates directly measured the potential of an electrolytic hydrogel submerged in an aqueous solution (Zheng and Pollack 2006; Shklyar et al. 2008). They observed the significant potential change only at the interface between the hydrogel and the bathing solution. Figure 18 illustrates the experimental system and the potential profile observed. Pollack et al. observed a drastic change in potential at the interface between the hydrogel and the electrolytic solution phase. The greater amount of cations must be adsorbed at the interface indicated by a dotted arrow in Fig. 18 and the greater number of positive charges of those cations must neutralize the immobile negative charges at the surface of the anionic hydrogel, and consequently, it must cause a drastic drop in potential at the interfacial region of the hydrogel. Of course, this hydrogel does not have any membrane, but its potential profile is explicable by ordinary thermodynamics and electromagnetism.

A cell consists of a greater quantity of charges possessed by the plasma membrane and proteins. Therefore, the nonzero potential is inevitably generated by those charges. We wonder why the ion channels and sodium pumps are needed for the membrane potential generation and, at the same time, why are thermodynamics and electromagnetism not considered to explain the membrane potential generation in the current physiology?

Membrane theory in the absence of physics and physical chemistry

When it comes to discussing life, we often hear scientific terminologies such as colloid, bound water, interface, and solubility of water, especially when discussing the origin of life (Bagatolli and Stock 2021; Bagatolli et al. 2021; Jaeken 2017; Matveev 2017, 2019; Galassi and Wilke 2021). Undoubtedly, these concepts are fundamental to the life sciences and every scientist must consider them as not negligible. However, they are not taken seriously in electrophysiological analysis and arguments. For example, the behaviour of a colloidal solution must, of course, conform to thermodynamics, but thermodynamics describes that the colloidal system is not in a thermodynamically ideal state, but in a thermodynamically real state (Katchalsky 1971). This is the same point of view as G. Ling, who is at the origin of AIH and has worked all his life to unify physiology and physics (Ling 1992; Ling 1997; Ling 2001; Ling 2007). However, it has not been well received by the mainstream physiological community until today because this view provides us with totally different physiological concepts that are in conflict with the membrane theory. Why cannot we be allowed to consider the physiological system as it is, i.e., as a thermodynamically real system? The currently accepted electrophysiological concepts are built on the thermodynamic view of the ideal system, but it is intuitively understandable that the thermodynamic view of the real system must be closer to the scientific truth. Ion adsorption is one element of activity change of the ion, and this theoretical treatment is within the conceptual range of a thermodynamically real system (Ling 1997; Lewis and Randall 1961). So, the occurrence of ion adsorption per se suggests the need to view the physiological system as a thermodynamically real system instead of a thermodynamically ideal system.

Recent physiological work by Bagatolli et al. is quite enlightening in that sense (Bagatolli and Stock 2021; Bagatolli et al. 2021). They argue for a thermodynamically realistic view of physiology and criticize the separation of physiology from physics and chemistry. They warn against reductionist methodologies in physiology, i.e., the neglect of the structure created by the mass of molecules, the disregard of its environment, the lack of consideration of the biological interface, the excess of plausible but thermodynamically unsupported physiological models, and the reliance on thermodynamically overidealized physiological experimental systems. Everything that Bagatolli et al. point out is perfectly rational as long as we researchers have a fair scientific mind. Schneider put forth a similar view, too, to the living system and attempted to unify the physiological facts and the foundation of physics, and his emphasis strongly roots, especially in thermodynamics (Schneider 2021). He does not necessarily criticise the current physiology but warns us

about the absence of physics in physiology. Quite intriguingly, his warning and the view of Bagatolli et al. have some in common. For example, Schneider has paid much attention to the cooperative phenomena occurring in the environment of mass of molecules. He also urges us to have a deeper perception of physiological phenomena and suggests that it will reveal more complex and fundamental natures of even the simple substances such as water and not only the proteins to be focused and important for physiology. The anomalous characteristics of water and its fundamental roles in the survival of life have been long discussed by Ling (Ling 1992; Ling 1997; Ling 2001; Ling 2007) and even at present deeply and precisely discussed by Pollack and his associates from the point of view of physical chemistry and physiology (Hwang et al. 2018; Pollack 2014; Wang and Pollack 2021). Jaeken discusses the derailment of physiology on the right track (Jaeken 2021). Just like Ling in his book (Ling 1997), Jaeken reflects on the history of physiology and touches upon the latest physiological work reported as early as 2020, then criticises the current physiology. So, he even more strongly warns us about the vulnerability of pressing forward physiological works unsupported by physics, such as Bagatolli et al. and Schneider warn (Bagatolli and Stock 2021; Bagatolli et al. 2021; Schneider 2021).

It seems that a number of researchers must have an unpleasant thought about physiology in the absence of physics and have not been able to fully accept it for many years.

Conclusions for future biology

Experimental evidence and theoretical considerations based on the electromagnetism suggest that the membrane potential generation does not require a nonzero membrane permeability. However, when it comes to the membrane potential in current electrophysiology, nonzero membrane permeability is a fundamental prerequisite for the induction of the membrane potential. There is something that does not work or is missing and is not considered in current electrophysiology. Yet, we have continually questioned the validity of the membrane theory until today (Tamagawa 2018; Tamagawa and Ikeda 2018; Tamagawa et al. 2021a, b). This doubt about the membrane potential generation mechanism, but also about electrophysiology itself, has been continuously raised by some research groups, even today (Hwang et al. 2018; Kowacz and Pollack 2020; Bagatolli and Stock 2021; Bagatolli et al. 2021; Manoj et al. 2019; Manoj and Jacob 2020; Manoj and Manekkathodi 2021). Although all physiology textbooks state that transmembrane ion transport is the origin of the membrane potential, we believe that there is a strong need to re-examine this issue. This is an unfinished research topic even today. As some researchers still suggest the problematic facets of current physiology in the absence

of physics, thermodynamics, we need to rethink physiological systems with the spirit of thermodynamics for a more real system. We believe that such an attitude allows totally new physiological results to emerge on their own.

AIH can explain the characteristics of potentials generated in a wide variety of systems even including the ISE and the dead cell. The AIH bears more universal facets than the membrane theory. The AIH foundation lies in the ordinary basic science such as thermodynamics, electromagnetism, statistical mechanics and physical chemistry. Compared with the membrane theory, the AIH is scientifically more rigid. Physiology has long been separated from the basic science and is derailed from the right track. No natural science can violate the laws of physics and physical chemistry. We should reconstruct the new physiology by unifying physiology and basic science.

Declarations

References

Bagatolli LA, Stock RP (2021) Lipids, membranes, colloids and cells: a long view. BBA Biomembranes. https://doi.org/10.1016/j.bbamem.2021.183684

Bagatolli LA, Mangiarotti A, Stock RP (2021) Cellular metabolism and colloids: realistically linking physiology and biological physical chemistry. Prog Biophys Mol Biol 162:79–88. https://doi.org/10.1016/j.pbiomolbio.2020.06.002

Barrow GM (1979) Physical chemistry. McGraw-Hill Inc., New York

Berg J (2021) An ion-selective electrode for detection of ammonium in wastewater treatment plants. Degree Project in Chemical Science and Engineering, Second Cycle, 30 Credits Stockholm, Sweden

Chang D (1983) Dependence of cellular potential on ionic concentrations. Data supporting a modification of the constant field equation. Biophys J 43(2):149–156. https://doi.org/10.1016/S0006-3495(83)84335-5

Cheng KL (1998) Explanation of misleading Nernst slope by Boltzmann equation. Microchem J 59:457–461. https://doi.org/10.1006/mchj.1998.1624

Cheng KL (2002) Recent development of non-faradaic potentiometry. Microchem J 72(3):269–276. https://doi.org/10.1016/S0026-265X(02)00092-9

Covington A (1981) Ion-selective electrodes. The Royal Society of Chemistry, London

Criscuolo F, Hanitra MIN, Taurino I, Carrara S, Micheli GD (2021) All-solid-state ion-selective electrodes: a tutorial for correct practice. IEEE Sens J 21(20):22143–22154. https://doi.org/10.1109/JSEN.2021.3099209

Cronin J (1987) Mathematical aspects of Hodgkin-Huxley neural theory. Cambridge University Press, New York

Diamond JM, Harrison SC (1966) The effect of membrane fixed charges on diffusion potentials and streaming potentials. J Physiol 183:37–57. https://doi.org/10.1113/jphysiol.1966.sp007850

Durst RA (Ed) (1969) Ion-selective electrodes. Institute for Materials Research National Bureau of Standards, Washington D.C

Ermentrout GB, Terman TH (2010) Mathematical foundations of neuroscience, vol 35. Interdisciplinary applied mathematics book. Springer, New York

Fischer RB (1974) Ion-selective electrodes. Proc California Assoc Chem Teach 51(6):387–390. https://doi.org/10.1021/ed051p387

Galassi VV, Wilke N (2021) On the coupling between mechanical properties and electrostatics in biological membranes. Membranes. https://doi.org/10.3390/membranes11070478

Hodgkin AL, Howrowicz P (1959) The influence of potassium and chloride ions on the membrane potential of single muscle fibers. J Physiol 148(1):127–160. https://doi.org/10.1113/jphysiol.1959.sp006278

Hwang SG, Hong JK, Sharma A, Pollack GH, Bahng GW (2018) Exclusion zone and heterogeneous water structure at ambient temperature. PLoS ONE. https://doi.org/10.1371/journal.pone.0195057

Jaeken L (2017) The neglected functions of intrinsically disordered proteins and the origin of life. Prog Biophys Mol Biol 126:31–46. https://doi.org/10.1016/j.pbiomolbio.2017.03.002

Jaeken L (2021) The greatest error in biological sciences, started in 1930 and continuing up to now, generating numerous profound misunderstandings. Curr Adv Chem Biochem 5:156–164. https://doi.org/10.9734/bpi/cacb/v5/1969F

Katchalsky A (1971) Polyelectrolytes. Pure Appl Chem 26(3–4):327–374. https://doi.org/10.1351/pac197126030327

Katoh T, Inda Y, Nakajima K, Ye R, Baba M (2010) Lithium/air batteries using Li-Ion conducting glass ceramics. ITE-IBA Lett Batter New Technol Med 3(4):327–374

Keener J, Sneyd J (2008) Mathematical physiology: I: cellular physiology. Interdisciplinary applied mathematics. Springer, New York

Kowacz M, Pollack GH (2020) Cells in new light: ion concentration, voltage, and pressure gradients across a hydrogel membrane. AOS Omega 5(33):21024–21031. https://doi.org/10.1021/acsomega.0c02595

Lewis GN, Randall M (1961) Thermodynamics. McGraw-Hill series in advanced chemistry, New York

Ling GN (1992) A revolution in the physiology of the living cell. Krieger Pub Co, Malabar

Ling GN (1997) Debunking the alleged resurrection of the sodium pump hypothesis. Physiol Chem Phys 29:123–198

Ling GN (2001) Life at the cell and below-cell level: the hidden history of a fundamental revolution in biology. Pacific Press, New York

Ling GN (2007) Nano-protoplasm: the Ultimate Unit of Life. Physiol Chem Phys & Med NMR 39:111–234

Manoj KM, Soman V, Jacob VD, Parashar A, Gideon DA, Kumar M, Manekkathodi A, Ramasamy S, Pakshirajan K, Bazhin NM (2019) Chemiosmotic and murburn explanations for aerobic respiration: predictive capabilities, structure-function correlations and chemico-physical logic. Arch Biochem Biophys. 676:108128. https://doi.org/10.1016/j.abb.2019.108128

Manoj KM, Jacob VD (2020) The murburn precepts for photoreception. Biomed Rev 31:67–74. https://doi.org/10.1016/j.jpap.2020.100015

Manoj KM, Manekkathodi A (2021) Light's interaction with pigments in chloroplasts: the murburn perspective. J Photochem Photobiol. 5:100015. https://doi.org/10.1016/j.jpap.2020.100015

Matveev V (2017) Comparison of fundamental physical properties of the model cells (protocells) and the living cells reveals the need in protophysiology. Int J Astrobiol 16(1):97–104. https://doi.org/10.1017/S1473550415000476

Matveev V (2019) Cell theory, intrinsically disordered proteins, and the physics of the origin of life. Prog Biophys Mol Biol 149:114–130. https://doi.org/10.1016/j.pbiomolbio.2019.04.001

Moreton RB (1968) An application of the constant-feld theory to the behaviour of giant neurons of the snail. Helix aspersa. J Exp Biol 48(3):611–662. https://doi.org/10.1242/jeb.48.3.611

Naik VA (2016) Principle and applications of ion selective electrodes-an overview. Int J Appl Res Sci Eng 2:2456–124X.

Olschewski A, Olschewski H, Bräu ME, Hempelmann G, Vogel W, Safronov BV (2001) Basic electrical properties of in situ endothelial cells of small pulmonary arteries during postnatal development. Am J Respir Cell Mol Biol 25:285–290. https://doi.org/10.1165/ajrcmb.25.3.4373

Pollack GH (2013) The fourth phase of water: beyond solid, liquid, and vapor. Edgescience 16:14

Pollack GH (2014) The fourth phase of water: beyond solid, liquid, and vapor. Ebner & Sons, Seattle

Radu A, Radu T, McGRAW C, Dillingham P, Anastasova-Ivanova S, Diamond D (2013) Ion selective electrodes in environmental analysis. J Serb Chem Soc 78(11):1729–1761. https://doi.org/10.2298/JSC130829098R

Rechnitz GA (1973) Mechanistic aspects of ion-selective membrane electrodes. A subjective view. Int Union Pure Appl Chem 5:457–471

Schneider MF (2021) Living systems approached from physical principles. Prog Biophys Mol Biol 162:2–25. https://doi.org/10.1016/j.pbiomolbio.2020.10.001

Shinagawa Y (1976) Physical basis of membrane potential (written in Japanese). Membrane (Japanese written journal) 1:176–183

Shklyar TF, Safronov AP, Klyuzhin IS, Pollack GH, Blyakhman FA (2008) A correlation between mechanical and electrical properties of the synthetic hydrogel chosen as an experimental model of Cytoskeleton. Biophysics 53(6):544–549. https://doi.org/10.1021/nn1018768

Tamagawa H, Ikeda K (2018) Another interpretation of Goldman-Hodgkin-Katz equation based on the Ling's adsorption theory. Eur Biophys J 47:869–879. https://doi.org/10.1007/s00249-018-1332-0

Tamagawa H (2018) Mathematical expression of membrane potential based on Ling's adsorption theory is approximately the same as the Goldman-Hodgkin-Katz equation. J Biol Phys 45(1):13–30. https://doi.org/10.1007/s10867-018-9512-9

Tamagawa H, Mulembo T, Delalande B (2021a) The need of the reconsideration of generation mechanism of membrane potential by mean of the Ling's adsorption theory. Eur Biophys J 50(6):793–803. https://doi.org/10.1007/s00249-021-01526-4

Tamagawa H, Mulembo T, Delalande B (2021b) What can S-shaped potential profiles tell us about the mechanism of membrane potential generation? Euro Biophys J 50(6):805–818. https://doi.org/10.1007/s00249-021-01531-7

Temsamani KR, Cheng KL (2001) Studies of chloride adsorption on the Ag/AgCl electrode. Sens Actuators B 76(1–3):551–555. https://doi.org/10.1016/S0925-4005(01)00624-4

Uteshev VV (2010) Evaluation of Ca2+ permeability of nicotinic acetylcholine receptors in hypothalamic histaminergic neurons. Acta Biochim Biophys Sin 42(1):8–20. https://doi.org/10.1093/abbs/gmp101

Wang A, Pollack GH (2021) Effect of infrared radiation on interfacial water at hydrophilic surfaces. Colloid Interface Sci Commun 42:100397. https://doi.org/10.1016/j.colcom.2021.100397

Wnek GE (2015) Perspective: do macromolecules play a role in the mechanisms of nerve stimulation and nervous transmission? J Polym Sci Part B Polym Phys 54(1):7–14. https://doi.org/10.1002/polb.23898

Wright EM, Diamond JM (1968) Efects of pH and polyvalent cations on the selective permeability of gall-bladder epithelium to monovalent ions. Biochim Biophys Acta 163(1):57–74. https://doi.org/10.1016/0005-2736(68)90033-3

Zhang X, Wakamatsu H (2002) A new equivalent circuit different from the Hodgkin-Huxley model, and an equation for the resting membrane potential of a cell. Artif Life Robot 6(3):140–148. https://doi.org/10.1007/BF02481329

Zheng J, Pollack GH (2006) Solute exclusion and potential distribution near hydrophilic surfaces. In: Pollack GH, Cameron IL, Wheatley DN (eds) Water and the Cell. Springer, Dordrecht